A&A 386, 916–925 (2002)
DOI: 10.1051/0004-6361:20020286

Astronomy & Astrophysics

Polarimetry of evolved stars

I. RS CVn and Mira variables

R. V. Yudin[1,2] and A. Evans[3]

[1] Central Astronomical Observatory of the Russian Academy of Sciences at Pulkovo, 196140 Saint-Petersburg, Russia
[2] Isaac Newton Institute of Chile, St.-Petersburg Branch, Russia
[3] Department of Physics, Keele University, Keele, Staffordshire, ST5 5BG, UK
e-mail: ae@astro.keele.ac.uk

Received 15 January 2002 / Accepted 25 February 2002

Abstract. We present broadband optical polarimetry of 3 RS CVn stars and 3 Mira variables, including the symbiotic star R Aqr, which contains a Mira component. Polarimetric variability has been studied on time-scales from hours to years. Our programme objects at the time of our observations showed different forms of $P(\lambda)$ dependence, $P \gtrsim \lambda^{-4}$ for most of the RS CVn-type stars, and $P \gtrsim \lambda^{-2}$ for the RS CVn-type star UV Psc and the Mira Ceti-type variables, and a significant increase of polarization to the red for the Mira R Cet. Combining our data with previously published data, we conclude that most of RS CVn-type and Mira Ceti-type objects show evidence of large polarimetric variability at wavelengths shorter than 0.5 μm, whereas the level of polarization is more stable in the red. This behaviour is consistent with episodic mass ejection and formation of small dust particles in the circumstellar environment. Although all targets showed polarimetric variability on different time scales, only for IM Peg might these variations be possibly linked with the photometric period.

Key words. polarization – circumstellar matter – stars: variables: general

1. Introduction

Polarimetry is a powerful observational tool that often allows one to determine the nature of stellar properties, and to pin down variability mechanisms. Photometric variability may of course have any one of a number of different origins: pulsation, the presence of cool or hot spots on the stellar surface, mass-transfer between components, the formation and dissipation of dusty and gaseous circumstellar (CS) envelopes, strong clumpiness of CS material due to episodic mass ejection, and eclipses. As several of these mechanisms may also give rise to polarimetric variations, polarimetric observations of these stars are highly desirable.

Although polarimetric observations of evolved stars were initiated many years ago (see, for example, the series of the papers by Serkowski 1966a,b; Kruszewski et al. 1968; Shawl 1975a,b), for many stars polarimetric data are rare or even non-existent. Although some objects have been intensively observed polarimetrically (for example the symbiotic star R Aqr (Schulte-Ladbeck 1985 and references therein)), several aspects of these stars remain unclear and any new data are likely to improve our knowledge and understanding of individual objects. On the other hand, it is important to study representative samples of the objects to enable us to establish common properties.

Unfortunately polarimetric investigations of even small samples of evolved stars are not numerous. For reference we note the papers of McCall & Hough (1980) on infrared (IR) polarimetry of 29 red giants and carbon stars; Schulte-Ladbeck & Magalhaes (1987) and Schulte-Ladbeck et al. (1990) on polarimetry of about 50 symbiotic stars, and the recent paper of Brandi et al. (2000 and references therein) for *UBVRI* polarimetry of 10 symbiotic stars. For the largest polarimetric data bank we note the paper of Serkowski & Shawl (2001), where *UBV* and *NORI* polarimetric data obtained over a 35-year period for 167 cool variables are catalogued.

In this series of papers we present polarization measurements of evolved stars with the aims of (i) studying the wavelength-dependence of polarization, (ii) investigating the temporal variability, on different time scales, on the $q - u$ diagram and comparing, where possible, with

Send offprint requests to: R. V. Yudin,
e-mail: ruslan61@hotmail.com

Table 1. List of the programme stars. Orbital periods from Berdyugina et al. (1999), Montesinos et al. (1988), Wilson et al. (1981).

Object	Other name	Sp class	Distance	Period		Comments
				Orbital	Photometric	
S Cet	HD 1987	M4e	1124 pc	–	$320\overset{\mathrm{d}}{.}45$	oxygen-rich Mira
UV Psc	HD 7700	G5V+K3III	63 pc	$0\overset{\mathrm{d}}{.}86104$	$0\overset{\mathrm{d}}{.}86$	eclipsing binary; RS CVn
R Cet	HD 15105	M4-M6e	760 pc	–	$166\overset{\mathrm{d}}{.}24$	Mira
IM Peg	HD 216489, H 8703	K1.5II-IIIe	97 pc	$24\overset{\mathrm{d}}{.}6488$	$24\overset{\mathrm{d}}{.}6$	RS CVn
SZ Psc	HD 219113	K1IV+F8IV	88 pc	$3\overset{\mathrm{d}}{.}96582$	$3\overset{\mathrm{d}}{.}96$	RS CVn
R Aqr	HD 222800, HR 8992	M7e+pec	197 pc	∼44 yr?	$\approx 386^{\mathrm{d}}$	symbiotic system containing Mira

previously published data, (iii) discussing briefly possible mechanisms that might be responsible for the observed behaviour.

2. Variables observed

In this paper we report observations of RS CVn and Mira variables. The stars observed are listed in Table 1; their basic characteristics including alternative names, spectral types, distances determined mainly from the Hipparcos parallaxes (Perryman et al. 1997) and photometric (and, where appropriate, orbital) periods are also listed.

A major shortcoming of many of the earlier polarimetric studies of cool stars is that little or no information on the exact JD dates of the observations and/or ephemerides used for calculations of phases is presented. For this reason we present in Table 2 photometric ephemerides for our programme stars, with references; the light curve phases ϕ in this paper are determined from the information in Table 2.

2.1. RS CVn variables

The RS CVn stars are active binaries, in which one component is a chromospherically active sub-giant. They often show radio and X-ray emission, and display persistent, quiescent, radio emission and frequently undergo radio "flares". The nature of the radio emission during flaring is well-known to be non-thermal (e.g. Dulk 1985), but the situation for the quiescent emission is unclear. V-band polarimetry of 30 RS CVn-type stars is reported by Liu & Tan (1987) – not easily accessible – while $UBVRI$ polarimetry of 15 RS CVn-type binaries is given by Scaltriti et al. (1993a).

2.2. Mira variables

Miras are long-period pulsating variables with large-amplitude variations in the visual/IR, and pulsational/photometric periods in the range ∼100–1000 days. Their high luminosities, and well-known period-luminosity relationship (e.g. Groenewegen & Whitelock 1996) make them valuable rungs on the cosmic distance ladder. They lie on the Asymptotic Giant Branch of the H-R diagram and, in common with objects at a similar phase of evolution, are are undergoing prolific mass-loss. They commonly form the cool component in symbiotic systems (Whitelock 1987).

3. Observations and analysis

The observations were carried out at the South African Astronomical Observatory (SAAO) during 1994 August 2–15, 1995 January 23–February 6 and 1995 July 18–August 31. The University of Cape Town (UCT) photometer-polarimeter module (Cropper 1985) was used on the SAAO 0.75 m telescope, although the observations for the period 1994 August 9–15 were carried out on the SAAO 1 m telescope. The instrumental linear and circular polarization, which has been measured by Clarke et al. (1998), was removed from our observational data. The observations were taken through $UBVR_{\mathrm{C}}I_{\mathrm{C}}$ filters; polarimetric standards were taken from the list of Hsu & Breger (1982). All observations were made with $20''$ aperture except one set, the $UBVR_{\mathrm{C}}I_{\mathrm{C}}$ data set for R Aqr on JD 49571.589–.606, when a $10''$ aperture was used.

The dataset is listed in Table 4, in which the Julian days are the time of mid-observation. The values of the normalized Stokes parameters (NSP) $q = Q/I$ and $u = U/I$ in Table 4 were corrected for instrumental polarization, noise bias etc. using the formalism of Clarke & Stewart (1986). Further details of the data analysis may be found in Yudin & Evans (1998) and Clarke et al. (1998). We tested for the presence of polarization using the $z-$statistic described in Clarke & Stewart (1986); where polarization was detected at the 99% ($\sim 3\sigma$) confidence level the values of the degree of polarization P and equatorial position angle θ are given in Table 4. The NSP (corrected for instrumental polarization) were also used to test for variability, using the Welch test (see Clarke & Stewart 1986). The detection level of circular polarization ($P_{\mathrm{circ}} \equiv v = V/I$) is shown in the last column in Table 4. Estimates of the visual magnitudes (with accuracy $\pm 0\overset{\mathrm{m}}{.}1$) of the programme stars, obtained with the UCT polarimeter, are also given in Table 4.

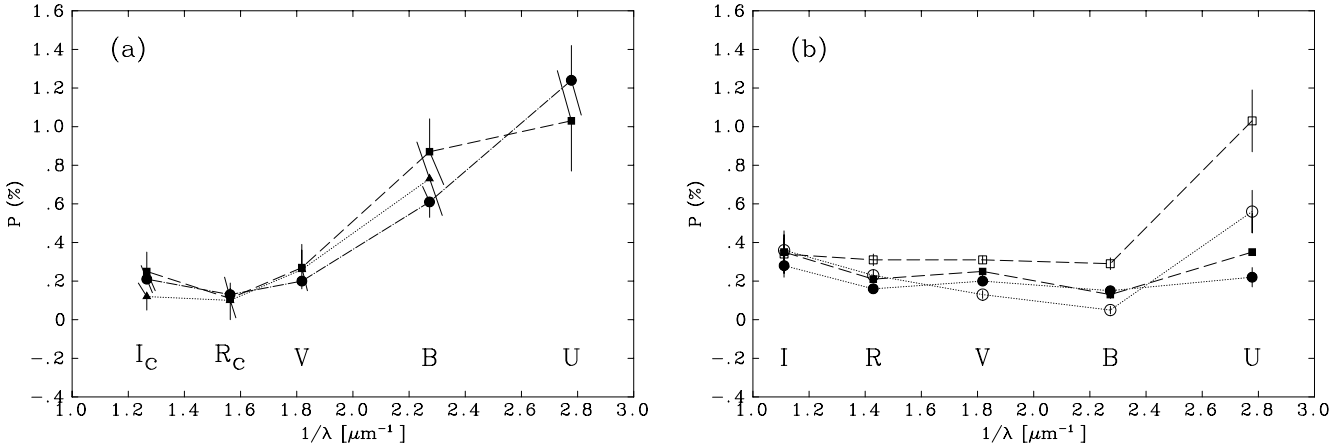

Fig. 1. a) Wavelength-dependence of polarization for IM Peg (triangles and dotted line), UV Psc (squares and dashed line), and SZ Psc (circles and dash-dot line). Data from this paper. **b)** Wavelength-dependence of polarization and its variability for the RS CVn star HD 199178 (squares and dashed lines) and RS CVn (circles and dotted lines). Note that the data for **b)** were obtained using Johnson filters and are from HPOL. Lines are included to guide the eye. See text for details.

Table 2. Photometric ephemerides of programme stars. "Min I" refers to the primary minimun in the light-curve.

Object	Ephemerides	Min/Max	Ref.
R Cet	$2443768.00 + 166.24 \times E$	Max	1
S Cet	$2442650.00 + 320.45 \times E$	Max	1
UV Psc	$2444932.2975 + 0.86104731 \times E$	Min I	2
IM Peg	$2450342.883 + 24.64880 \times E$	Min	3
SZ Psc	$2444827.0047 + 3.9657889 \times E$	Min I	4
R Aqr	$2444733.76 + 385.509 \times E$	Max	5

(1) Kholopov et al. (1998); (2) Sowell et al. (2001); (3) Berdyugina et al. (1999); (4) Kalimeris et al. (1995); (5) Chinarova et al. (1996).

4. Discussion of individual objects

4.1. RS CVn-type stars

4.1.1. IM Peg

Six V-band polarimetric measurements published previously by Liu & Tan (1987) showed a low level of polarization for this star (≈0.1%–0.15%). According to the ephemerides taken from Berdyugina et al. (1999) we observed IM Peg near minimum light ($\phi \approx 0.91$), corresponding well to our V-band photometry ($m_V \approx 6\overset{\mathrm{m}}{.}1$). In our measurements the object showed a low (≃0.1%) level of polarization in the $VR_{\rm C}I_{\rm C}$ bands but with a clear increase of P to shorter wavelengths (see Fig. 1a).

We have attempted to estimate the interstellar (IS) component of polarization in the V-band using the catalogue of Heiles (2000). Our study of IS polarization in the vicinity of IM Peg leads to the estimate $P_{\rm is} = 0.08 \pm 0.02\%$ at $\theta_{\rm is} = 100° \pm 5°$; as the distance of IM Peg is so small any correction of the observational data for the IS component does not change the wavelength-dependence. As noted by Scaltriti et al. (1993a) and Vasil'ev et al. (1993), most objects of this type usually show a low level of $UBVRI$ polarization, with flat wavelength-dependence. For IM Peg, however, the wavelength-dependence of polarization corresponds well with the Rayleigh law, $P \propto \lambda^{-4}$, possibly indicating scattering by small particles or molecules in a CS envelope when the system is at minimum light. Similar wavelength-dependence of polarization is sometimes seen in symbiotic stars and in Mira variables (see, for example, Schulte-Ladbeck et al. 1990; Brandi et al. 2000). Although Donati et al. (1997) noted the possible detection of circular polarization for IM Peg at phase ≈0.39, no circular polarization is detected, within the errors, in our study. Combining our data with those obtained by Liu & Tan (1987), we conclude that the V-band polarization decreases to zero at maximum light, and reaches ≃0.2% in the minima.

4.1.2. UV Psc

Polarimetric data for this object have been obtained on one occasion in the $UBVR_{\rm C}$ bands. Previous polarimetric observations of UV Psc by Scaltriti et al. (1993a) and by Liu & Tan (1987) show low polarization in the $UBVR$ bands at a level of about 0.1%, with a possible increase to 0.2% in I. The values reported here are in agreement with those obtained by Scaltriti et al. and by Liu & Tan for the polarization in the VRI bands, but is significantly higher in UB (however we should note that these authors' observations were obtained using Johnson VRI filters, in contrast to our Cousins $VR_{\rm C}I_{\rm C}$). As with IM Peg, this object shows a clear increase of polarization to shorter wavelengths, up to a value ≃1% in the U-band. The wavelength-dependence of polarization is well described by $P \propto \lambda^{-2}$ (see Fig. 1a).

Note that UV Psc is the nearest object in our study, so the IS polarization in the V-band does not exceed 0.05%, with $\theta_{\rm is} \approx 125°$; these values follow from our

investigation of the $P_{\rm is} - D$ relation, constructed using the catalog of Heiles (2000). Our observations were obtained at phase $\phi \sim 0.25$–0.26, i.e. when the system was midway between primary and secondary minima (see, for example, the light curve in Han & Kim 1988) and was bright ($m_V \approx 9\overset{\rm m}{.}0$). Most of the observations by Scaltriti et al. (1993a) and by Liu & Tan (1987) were also obtained close to maximum light, i.e. between eclipses. No correlations were found between the degree of polarization and phase variations. Within the errors, no circular polarization has been detected for this object.

4.1.3. SZ Psc

As with the above stars, SZ Psc exhibits low polarization in the $VR_{\rm C}$ bands ($\simeq$0.1%–0.2%), with possibly a small increase in $I_{\rm C}$, and a significant rise to the UB bands (up to 1%). This behaviour was not observed in the 1991 $UBVRI$ observations of Vasil'ev et al. (1993), obtained in one day. These authors noted a flat wavelength-dependence, with polarization about 0.1% in UB and a slight increase of polarization in VRI (up to 0.2%). Note, however, that in three of the four observations of Liu & Tan (1987) the V-band polarization of this object was about 0.6%–0.7%. The distance of SZ Psc suggests a degree of IS polarization $P_{\rm is} \simeq 0.14 \pm 0.02\%$ at $\theta_{\rm is} = 106^\circ \pm 2^\circ$. Our measurements, together with those of Vasil'ev et al. (1993) and Liu & Tan (1987), are depicted in the qu-plane in Fig. 2. As may be seen from this figure, intrinsic polarization for this star is present at the $\gtrsim$99% confidence level for all measurements, except our one V-band datum for JD 917.541 (note that, taking into account *interstellar* polarization, an *observed* polarization that is indistinguishable from zero does not indicate the absence of *intrinsic* polarization). Polarimetric variability was detected at the 99.9% confidence level for our $VR_{\rm C}$ measurements.

To study the wavelength-dependence of polarization we used our average data obtained in 1994 (when 5-colour polarimetry was carried out) for each of the passbands. After subtracting the IS component we obtain the values of intrinsic polarization in Table 3.

The wavelength-dependence is well approximated by the law $P \gtrsim \lambda^{-4}$ (see Fig. 1a), close to the Rayleigh law. Note that the position angle of intrinsic polarization changes from the U to the $I_{\rm C}$ band, possibly indicating that different zones in the envelope are responsible for polarization in the UV and in the red. If (as in Table 3), we add the 1995 data in the $VR_{\rm C}I_{\rm C}$ bands, the level of *intrinsic* polarization is not affected but the differences in the *intrinsic* position angle between UBV and $R_{\rm C}I_{\rm C}$ becomes more pronounced.

Although our two data sets correspond to different phases ($\phi \simeq 0.37, 0.38$ and 0.61 for 1994 and 1995 respectively) they both lie near maximum light, and between eclipses (see Figs. 3 and 5 of Lanza et al. 2001). Three measurements of Liu & Tan (1987) with $P \approx 0.6$–0.7% were obtained at phases $\approx$0.6–0.8 but their last observation, at phase 0.09 (i.e. close to minimum), showed a decrease of P to 0.17%. This behaviour is unusual, but the available bank of data is still not enough to draw any conclusions on a link between photometric variations and polarization.

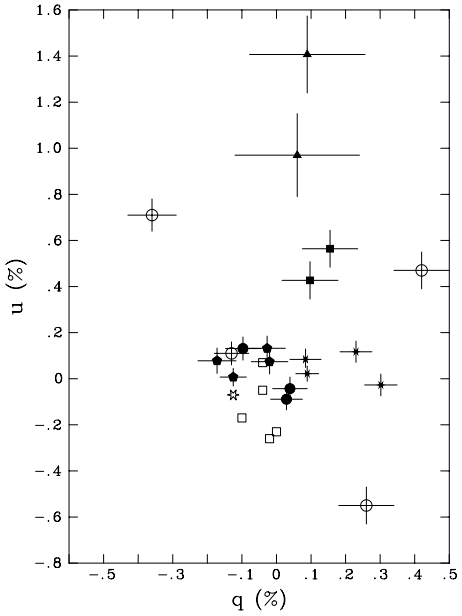

Fig. 2. Polarimetric variations in the qu plane for SZ Psc. Filled symbols are data from this paper: triangles, U-band, squares, B-band, pentagons, V-band; circles, $R_{\rm C}$-band; stars, $I_{\rm C}$-band measurements. Open squares: $UBVRI$ data from data from Vasil'ev et al. (1993). Open circles; V-band data from Liu & Tan (1987). Open star is estimate of IS polarization.

Donati et al. (1997), from their spectropolarimetric observations, reported the detection of circular polarization for this object at photometric phases 0.182, 0.195 and 0.208, at the 15σ level. In previous observations of SZ Psc by Donati et al. (1992), at phases 0.611 and 0.624, circular polarization was not detected. Our observations show detectable (at the $\approx 3\sigma$ level) circular polarization on JD 917 (i.e. at phase 0.61). It is also noteworthy that the values of $P_{\rm circ}$ are persistently negative, with an overall weighted mean of $-0.027\% \pm 0.012\%$.

4.1.4. Comments on RS CVn-type stars

We note that all three objects of this type show similar wavelength-dependence of polarization, with a clear increase in P toward shorter wavelengths. This behaviour can not be accounted for by inappropriate treatment of data (e.g. incorrect allowance for instrumental and IS polarization). Even if the values of instrumental polarization used for the reduction in the UBV bands are overestimated, the values of observed polarization (i.e. uncorrected for the instrumental component) clearly show the same law. However, the increase of P in the UB bands seems not to be typical for RS CVn-type stars. Only one object (II Peg) among the 20 stars from the

Table 3. Intrinsic polarization for SZ Psc for 1994 data only, and averaged over 1994+1995 data.

1994 only		1994+1995	
$P_U = 1.22 \pm 0.18\%$	$\theta_U = 41^\circ \pm 5^\circ$	$P_U = 1.22 \pm 0.18\%$	$\theta_U = 41^\circ \pm 5^\circ$
$P_B = 0.61 \pm 0.08\%$	$\theta_B = 34^\circ \pm 3^\circ$	$P_B = 0.61 \pm 0.08\%$	$\theta_B = 34^\circ \pm 3^\circ$
$P_V = 0.20 \pm 0.03\%$	$\theta_V = 31^\circ \pm 4^\circ$	$P_V = 0.15 \pm 0.03\%$	$\theta_V = 39^\circ \pm 5^\circ$
$P_{R_C} = 0.15 \pm 0.03\%$	$\theta_{R_C} = 27^\circ \pm 8^\circ$	$P_{R_C} = 0.13 \pm 0.04\%$	$\theta_{R_C} = 17^\circ \pm 8^\circ$
$P_{I_C} = 0.26 \pm 0.07\%$	$\theta_{I_C} = 16^\circ \pm 8^\circ$	$P_{I_C} = 0.30 \pm 0.08\%$	$\theta_{I_C} = 11^\circ \pm 8^\circ$

Scaltriti et al. and Vasil'ev et al. programmes shows such behaviour, but at a significantly smaller level of polarization ($P_U \approx 0.08\%$). We were gratified to find similar polarimetric data for two other RS CVn-type stars, HD 199178 and RS CVn itself, in the HPOL database (see `www.sal.wisc.edu/HPOL/`) and in Pfeiffer (1979). These stars both display temporal variability of the $P(\lambda)$ dependence, from flat at longer wavelengths and increasing to the ultraviolet (see for example, Fig. 1b). Thus, the $P(\lambda)$ behaviour reported here seems real.

To explain the wavelength-dependence for II Peg, Scaltriti et al. (1993a) suggested scattering either from small dust particles or from molecules. According to Scaltriti et al. (1993b) there is an optically thin CS dust shell around II Peg, as evidenced by an IR excess, and about half of the RS CVn-type stars studied by Scaltriti et al. show evidence of optically thin CS dust envelopes. However, although IM Peg shows detectable fluxes in the IR up to $\lambda = 25\,\mu$m, for UV Psc and SZ Psc the far-IR fluxes were detected only at $\lambda = 12\,\mu$m and at a significantly smaller level, and no near-IR data have been published for them.

On the other hand, SZ Psc is a strongly spotted system. From Lanza et al. (2001), the total spotted area of the K1 IV secondary in this system was about 20–25% at the time of our observations. The presence of numerous spots can lead to the observed wavelength-dependence of polarization at the level detected (see, for example, Schwarz & Clarke 1984).

Finally, UV Psc is one of the short-period ($0\overset{\mathrm{d}}{.}86$) binaries and there is much evidence of mass-transfer from the cooler component in this system (Hall & Ramsey 1994; Welty & Ramsey 1995). When the components of the system are located in the plane of the sky (corresponding to our observations at phase 0.37–0.38 at JD 575–579), there are important consequences for observing specific features of the system, such as gas streams and the effect of stellar nonsphericity, also observable at phases 0.3 and 0.7. Note that light fluctuations take place in the UV Psc system outside eclipses, whereas photometric parameters of the minima are very similar (see, for example Han & Kim 1988). This behaviour can be a consequence of variable mass flow, although to explain it Jassur & Kermani (1994) suggested the presence of cool spots on the surface of the primary component. Our data are insufficient to distinguish between these mechanisms.

4.2. Mira Ceti variables

4.2.1. S Cet

No polarimetric measurements have previously been reported for S Cet. Our polarimetric observations of this star were obtained on two consecutive nights, i.e. effectively at one phase of brightness variations (the photometric period is $320\overset{\mathrm{d}}{.}8$). Although the mean data for two nights are indistinguishable one from another, polarimetric differences in the VR_C bands during the first night are evident at the 95% confidence level. Assuming a distance to the object of about 1100 pc, the IS component of polarization in the V-band is $P_{\rm is} \approx 0.2\%$ at $\theta_{\rm is} \approx 135^\circ$. After subtracting $P_{\rm is}$, the calculated level of intrinsic polarization is about 0.3%–0.7%. The wavelength dependence of intrinsic polarization is plotted in Fig. 3. We see that the decrease of polarization to the red is described by the law $P(\lambda) \propto \lambda^{-2}$. This is typical for this class of object (see, for example, Kruszewski et al. 1968), and is explained in terms of scattering by dust particles with a range of sizes in an asymmetric CS envelope. A detectable (at the 2–4σ confidence level) circular polarization was found in the R_C-band on JD923, and it has the same sign on the following date.

4.2.2. R Cet

Only one *UB* measurement of this star was made by Serkowski & Shawl (2001) and it shows polarization at the level of about 1–2% (the error in the U-band was, however, very large). From our data we conclude that the polarization degree increases to the red (see Fig. 3) from $\approx$0.1% in the V-band to $\approx$0.4% in the I_C-band. This is a clear indication of scattering by large dust particles in a CS envelope. The IS component of polarization seems to be negligible for this star, as it located at high Galactic latitude. However, should it be non-negligible, its subtraction would make the wavelength behaviour even more pronounced.

4.2.3. R Aqr: An unusual symbiotic star

R Aqr is a puzzling system that is suggested to contain a mass-losing Mira variable, a hot companion/accretion disc, a dust shell, a bipolar nebula, and an inner "jet-like" structure (see e.g. Hollis et al. 1997 and references

Table 4. Polarimetric data for RS CVn and Mira variables.

Object ϕ	JD 2 449 000+	Filter	m_V	q (%)	u (%)	P (%)	θ (°)	v (%)	P_c level
IM Peg	576.508	U		-0.34 ± 0.65	0.04 ± 0.65	0.34 ± 0.65	86 :	-0.501 ± 0.462	
	576.510	B		-0.25 ± 0.19	0.68 ± 0.19	0.72 ± 0.19	55.0 ± 7.6	-0.113 ± 0.132	
0.91	576.510	V	6.1	-0.02 ± 0.10	0.23 ± 0.10	0.23 ± 0.10	47.9 ± 12.5	0.017 ± 0.071	
	576.511	R_C		-0.06 ± 0.09	0.07 ± 0.09	0.09 ± 0.09	67.3 ± 20.7	0.018 ± 0.061	
	576.512	I_C		0.06 ± 0.07	0.01 ± 0.07	0.06 ± 0.07	6 ± 22	0.063 ± 0.051	
UV Psc	579.587	U		0.29 ± 0.26	0.96 ± 0.26	0.96 ± 0.26	36.2 ± 7.9	-0.251 ± 0.186	
	579.594	B		0.13 ± 0.17	0.82 ± 0.17	0.83 ± 0.17	40.4 ± 5.9	-0.077 ± 0.119	
0.25–	579.595	V	9.0	-0.25 ± 0.12	0.09 ± 0.12	0.27 ± 0.12	80.1 ± 12.6	-0.082 ± 0.082	
0.26	579.596	R_C		0.07 ± 0.11	0.04 ± 0.11	0.08 ± 0.11	13:	0.030 ± 0.080	
	579.597	I_C		0.20 ± 0.10	0.11 ± 0.10	0.23 ± 0.10	14.5 ± 13.4	0.106 ± 0.075	
SZ Psc	575.520	U		0.089 ± 0.167	1.407 ± 0.167	1.410 ± 0.167	43.0 ± 3.4	0.008 ± 0.118	
	575.525	B		0.097 ± 0.081	0.427 ± 0.081	0.438 ± 0.081	38.6 ± 5.3	-0.035 ± 0.057	
0.37	575.526	V	7.3	-0.020 ± 0.053	0.074 ± 0.053	0.077 ± 0.053	52.6 ± 19.7	0.001 ± 0.038	
	575.527	R_C		0.039 ± 0.050	-0.043 ± 0.050	0.058 ± 0.050	156.1 ± 24.7	0.019 ± 0.035	
	575.528	I_C		0.230 ± 0.046	0.117 ± 0.046	0.258 ± 0.046	13.5 ± 5.1	0.005 ± 0.032	
	579.532	U		0.06 ± 0.18	0.97 ± 0.18	0.97 ± 0.18	43.2 ± 5.3	-0.050 ± 0.126	
	579.533	B		0.155 ± 0.080	0.564 ± 0.080	0.580 ± 0.080	37.4 ± 1.4	0.011 ± 0.057	
0.38	579.534	V	7.3	-0.027 ± 0.053	0.132 ± 0.053	0.135 ± 0.053	50.8 ± 11.2	-0.008 ± 0.037	
	579.535	R_C		-0.097 ± 0.050	0.131 ± 0.050	0.163 ± 0.050	63.3 ± 8.8	-0.009 ± 0.035	
	579.536	I_C		0.084 ± 0.045	0.084 ± 0.045	0.119 ± 0.045	22.5 ± 10.8	-0.013 ± 0.032	
	917.529	V	7.4	-0.172 ± 0.055	0.078 ± 0.055	0.189 ± 0.055	77.8 ± 8.3	0.030 ± 0.039	
0.38	917.531	R_C		0.029 ± 0.046	-0.089 ± 0.046	0.094 ± 0.046	144.0 ± 14.0	-0.057 ± 0.032	1.8σ
	917.532	I_C		0.302 ± 0.047	-0.027 ± 0.047	0.303 ± 0.047	177.4 ± 4.4	-0.094 ± 0.033	2.8σ
	917.541	V	7.4	-0.125 ± 0.038	0.007 ± 0.038	0.125 ± 0.038	88.4 ± 8.7	-0.078 ± 0.027	3.4σ
	917.548	I_C		0.089 ± 0.033	0.022 ± 0.033	0.092 ± 0.033	6.9 ± 10.3	0.000 ± 0.023	
S Cet	923.617	V	10.7	0.738 ± 0.122	-0.167 ± 0.122	0.762 ± 0.122	173.6 ± 4.6	-0.157 ± 0.086	1.8σ
	923.624	R_C		0.313 ± 0.057	-0.264 ± 0.057	0.409 ± 0.057	159.9 ± 4.0	-0.159 ± 0.040	4.0σ
	923.631	I_C		0.361 ± 0.027	-0.145 ± 0.027	0.389 ± 0.027	169.1 ± 2.0	0.000 ± 0.019	
0.70	923.650	V	10.7	0.497 ± 0.123	-0.356 ± 0.123	0.611 ± 0.123	162.2 ± 5.8	0.024 ± 0.087	
	923.657	R_C		0.374 ± 0.058	-0.011 ± 0.057	0.374 ± 0.058	179.2 ± 4.4	-0.087 ± 0.041	2.1σ
	923.664	I_C		0.353 ± 0.027	-0.139 ± 0.027	0.379 ± 0.027	169.3 ± 2.0	-0.027 ± 0.019	
0.70	924.631	V	10.6	0.590 ± 0.110	-0.310 ± 0.110	0.666 ± 0.110	166.1 ± 4.7	-0.035 ± 0.078	
	924.638	R_C		0.394 ± 0.053	-0.305 ± 0.053	0.498 ± 0.053	161.1 ± 3.0	0.009 ± 0.038	
	924.645	I_C		0.289 ± 0.027	-0.151 ± 0.027	0.326 ± 0.027	166.2 ± 2.4	0.016 ± 0.019	
R Cet	926.639	V	8.6	0.116 ± 0.047	0.107 ± 0.047	0.157 ± 0.047	21.4 ± 8.6	0.016 ± 0.018	
0.05	926.646	R_C		0.245 ± 0.026	0.084 ± 0.026	0.259 ± 0.026	9.4 ± 2.9	0.027 ± 0.033	
	926.651	I_C		0.395 ± 0.014	-0.001 ± 0.014	0.395 ± 0.014	179.9 ± 1.0	-0.003 ± 0.010	
R Aqr	571.580	V	10.6	0.24 ± 0.21	-2.751 ± 0.21	2.76 ± 0.21	132.6 ± 2.2	-0.180 ± 0.150	
0.55	571.581	R_C		-0.05 ± 0.06	-0.858 ± 0.06	0.86 ± 0.06	133.2 ± 1.9	0.007 ± 0.041	
	571.585	I_C		0.71 ± 0.20	-0.437 ± 0.20	0.83 ± 0.20	164.1 ± 6.8	0.132 ± 0.139	
	575.600	U		-0.28 ± 0.66	-5.53 ± 0.66	5.54 ± 0.66	133.5 ± 4.9	0.097 ± 0.467	
	575.601	B		-0.60 ± 0.41	-5.12 ± 0.41	5.16 ± 0.41	131.7 ± 3.1	-0.057 ± 0.292	
0.56	575.603	V	10.4	-0.75 ± 0.22	-3.29 ± 0.22	3.38 ± 0.22	128.6 ± 3.2	-0.192 ± 0.158	
	575.604	R_C		0.20 ± 0.08	-0.87 ± 0.08	0.90 ± 0.08	141.4 ± 5.1	-0.022 ± 0.055	
	575.610	I_C		0.41 ± 0.29	-0.41 ± 0.29	0.58 ± 0.29	157.4 ± 19.8	-0.005 ± 0.208	
	576.566	U		-1.42 ± 0.62	-4.22 ± 0.62	4.45 ± 0.62	125.7 ± 7.3	0.095 ± 0.435	
	576.568	B		-0.78 ± 0.32	-3.85 ± 0.32	3.93 ± 0.32	129.2 ± 3.2	0.165 ± 0.227	
0.56	576.570	V	10.4	0.03 ± 0.21	-2.65 ± 0.21	2.65 ± 0.21	135.3 ± 4.4	-0.017 ± 0.145	
	576.571	R_C		0.23 ± 0.07	-0.94 ± 0.07	0.97 ± 0.07	141.9 ± 4.0	0.054 ± 0.046	
	576.573	I_C		0.51 ± 0.02	-0.43 ± 0.02	0.66 ± 0.02	159.8 ± 4.4	0.012 ± 0.016	

Table 4. continued.

Object ϕ	JD 2 449 000+	Filter	m_V	q (%)	u (%)	P (%)	θ (°)	v (%)	P_c level
R Aqr	576.589	U		0.49 ± 1.04	-7.13 ± 1.04	7.14 ± 1.04	137.0 ± 4.4	-0.446 ± 0.741	
(10″)	576.591	B		-0.29 ± 0.50	-4.70 ± 0.50	4.71 ± 0.50	133.2 ± 5.0	0.497 ± 0.358	
	576.594	V		-0.22 ± 0.23	-2.56 ± 0.23	2.57 ± 0.23	132.5 ± 5.0	0.097 ± 0.163	
	576.595	R_C		0.27 ± 0.09	-0.90 ± 0.09	0.94 ± 0.09	143.4 ± 5.6	0.115 ± 0.064	1.8σ
R Aqr	579.550	U		-1.34 ± 0.68	-4.58 ± 0.68	4.78 ± 0.68	126.8 ± 4.1	0.299 ± 0.482	
(20″)	579.552	B		-0.18 ± 0.43	-4.60 ± 0.43	4.60 ± 0.43	133.9 ± 2.7	-0.146 ± 0.305	
0.57	579.553	V	10.5	-0.44 ± 0.23	-2.65 ± 0.23	2.68 ± 0.23	130.3 ± 2.5	-0.118 ± 0.165	
	579.554	R_C		0.233 ± 0.082	-0.764 ± 0.082	0.799 ± 0.082	143.5 ± 2.9	0.015 ± 0.058	
	579.555	I_C		0.485 ± 0.026	-0.368 ± 0.026	0.609 ± 0.026	161.4 ± 1.2	0.016 ± 0.018	
0.45	918.551	V	9.8	0.525 ± 0.380	-2.080 ± 0.380	2.150 ± 0.380	142.1 ± 5.1	0.036 ± 0.059	
	918.554	R_C		0.674 ± 0.118	-0.284 ± 0.118	0.731 ± 0.118	168.6 ± 4.6	0.483 ± 0.083	5.8σ
	918.560	I_C		0.710 ± 0.042	-0.367 ± 0.042	0.799 ± 0.042	166.3 ± 1.5	0.031 ± 0.030	
0.46	922.541	V	9.9	0.517 ± 0.083	-2.082 ± 0.083	2.145 ± 0.083	142.0 ± 1.1	0.036 ± 0.059	
	922.548	R_C		0.742 ± 0.034	-0.675 ± 0.034	1.003 ± 0.038	158.9 ± 1.1	-0.092 ± 0.024	2.1σ
	922.555	I_C		0.669 ± 0.014	-0.488 ± 0.014	0.828 ± 0.014	161.9 ± 0.5	0.025 ± 0.010	2.5σ
	923.526	V	10.0	0.585 ± 0.083	-1.983 ± 0.083	2.067 ± 0.083	143.3 ± 1.2	-0.007 ± 0.006	
	923.536	R_C		0.587 ± 0.027	-0.789 ± 0.027	0.983 ± 0.027	153.3 ± 0.8	0.017 ± 0.019	
	923.543	I_C		0.599 ± 0.010	-0.514 ± 0.010	0.789 ± 0.010	159.7 ± 0.4	0.005 ± 0.007	
0.46	923.564	V	9.9	0.684 ± 0.083	-1.945 ± 0.083	2.062 ± 0.083	144.7 ± 1.2	-0.054 ± 0.059	
	923.571	R_C		0.659 ± 0.027	-0.724 ± 0.027	0.979 ± 0.027	156.2 ± 0.8	0.027 ± 0.019	
	923.578	I_C		0.591 ± 0.010	-0.525 ± 0.010	0.791 ± 0.010	159.2 ± 0.4	0.020 ± 0.007	2.9σ
0.46	924.537	V	9.8	0.557 ± 0.078	-1.844 ± 0.078	1.926 ± 0.078	143.4 ± 1.2	0.074 ± 0.056	
	924.544	R_C		0.640 ± 0.025	-0.811 ± 0.025	1.033 ± 0.025	154.1 ± 0.7	-0.010 ± 0.018	
	924.551	I_C		0.613 ± 0.010	-0.480 ± 0.010	0.779 ± 0.010	161.0 ± 0.4	-0.005 ± 0.007	
	926.524	V	9.9	0.520 ± 0.106	-1.946 ± 0.106	2.014 ± 0.106	142.5 ± 1.5	-0.103 ± 0.075	
	926.528	R_C		0.599 ± 0.034	-0.757 ± 0.034	0.965 ± 0.034	154.2 ± 1.0	0.021 ± 0.024	
	926.535	I_C		0.628 ± 0.013	-0.504 ± 0.013	0.805 ± 0.013	160.6 ± 0.5	0.013 ± 0.015	
0.47	926.546	V	9.9	0.215 ± 0.265	-2.180 ± 0.265	2.190 ± 0.265	137.8 ± 1.5	-0.388 ± 0.182	2.1σ
	926.553	R_C		0.698 ± 0.082	-0.900 ± 0.082	1.138 ± 0.082	153.9 ± 1.0	0.125 ± 0.058	2.2σ
	926.556	I_C		0.628 ± 0.021	-0.504 ± 0.021	0.805 ± 0.013	160.6 ± 0.5	0.013 ± 0.015	
	927.523	V	9.9	0.475 ± 0.082	-1.862 ± 0.082	1.922 ± 0.082	142.2 ± 1.2	-0.203 ± 0.058	3.5σ
	927.530	R_C		0.607 ± 0.027	-0.829 ± 0.027	1.027 ± 0.027	153.1 ± 0.8	0.055 ± 0.019	2.9σ
0.47	927.537	I_C		0.591 ± 0.010	-0.529 ± 0.010	0.793 ± 0.010	159.1 ± 0.4	-0.003 ± 0.007	
	927.593	V	10.0	0.548 ± 0.089	-1.935 ± 0.089	2.011 ± 0.089	142.9 ± 1.1	0.175 ± 0.063	2.8σ
	927.600	R_C		0.575 ± 0.037	-0.816 ± 0.037	0.998 ± 0.037	152.6 ± 1.1	0.014 ± 0.026	
	929.521	V	10.0	0.694 ± 0.087	-2.169 ± 0.087	2.277 ± 0.087	143.9 ± 1.1	-0.005 ± 0.060	
	929.528	R_C		0.796 ± 0.094	-1.157 ± 0.094	1.405 ± 0.094	152.3 ± 1.1	0.359 ± 0.066	5.4σ
	929.548	V	10.0	0.466 ± 0.085	-2.248 ± 0.085	2.296 ± 0.085	140.9 ± 1.0	0.101 ± 0.060	
	929.555	R_C		0.609 ± 0.029	-0.747 ± 0.029	0.964 ± 0.029	154.6 ± 0.9	0.057 ± 0.021	2.7σ
0.48	929.564	I_C		0.615 ± 0.037	-0.571 ± 0.037	0.839 ± 0.037	158.6 ± 1.3	-0.006 ± 0.026	
	929.576	V	10.1	0.834 ± 0.095	-2.095 ± 0.095	2.255 ± 0.095	145.9 ± 1.2	0.100 ± 0.067	
	929.583	R_C		0.584 ± 0.034	-0.829 ± 0.034	1.014 ± 0.034	152.6 ± 1.0	0.029 ± 0.024	
	929.591	I_C		0.533 ± 0.038	-0.477 ± 0.38	0.715 ± 0.038	159.1 ± 1.5	-0.018 ± 0.027	
	930.548	V		0.779 ± 0.182	-1.752 ± 0.182	1.917 ± 0.182	147.0 ± 1.0	0.269 ± 0.129	2.1σ
	930.555	R_C		0.677 ± 0.052	-0.701 ± 0.052	0.974 ± 0.052	157.0 ± 0.9	0.044 ± 0.037	
	930.564	I_C		0.543 ± 0.033	-0.493 ± 0.033	0.734 ± 0.033	158.9 ± 1.3	0.059 ± 0.023	2.6σ
0.48	930.576	V		0.622 ± 0.141	-2.025 ± 0.141	2.119 ± 0.141	143.5 ± 1.2	0.025 ± 0.100	
	930.583	R_C		0.727 ± 0.034	-0.722 ± 0.034	1.025 ± 0.034	157.6 ± 1.0	0.029 ± 0.024	
	930.591	I_C		0.638 ± 0.014	-0.470 ± 0.14	0.792 ± 0.014	161.8 ± 1.5	0.001 ± 0.010	

therein). In spite of the long history of study using the largest telescopes (Keck I: Tuthill et al. 2001; MMT: Karovska et al. 1994; VLA, BIMA, VLBA: Hollis et al. 2000, 2001), its nature and physical parameters remain unclear and sometimes controversial. Tuthill et al. (2001), in contrast to the conclusions of Karovska et al. (1994), do not find evidence of elongation of the CS envelope along position angle $\theta \approx 140°$. In addition, no evidence for the presence of a companion separated by more than ∼15 mas was found by them, but a significant deviation from circular symmetry of the CS dust envelope was reported. Hollis et al. (2001) reported that the axis of rotational

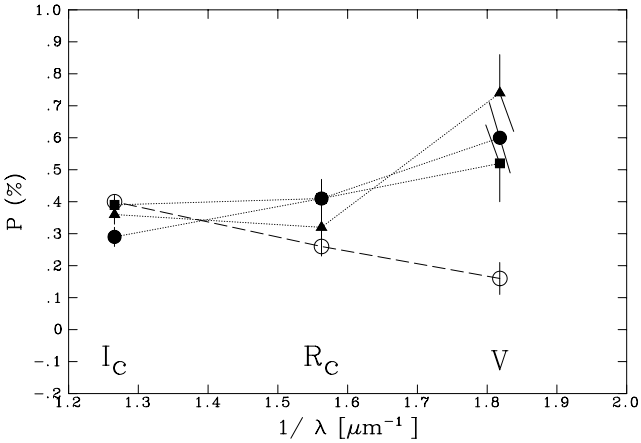

Fig. 3. Wavelength-dependence of polarization for R Cet (open circles) and S Cet (filled symbols); triangles, JD...923.6, squares, JD...923.7, circles, JD...924. Lines are included to guide the eye.

Table 5. Wavelength-dependence of position angle from 1994–1995 for R Aqr.

Season	θ_U/σ	θ_B/σ	θ_V/σ	θ_{R_C}/σ	θ_{I_C}/σ
1994	131°	132°	132°	141°	161°
	2°	1°	1°	2°	1°
1995			143°	156°	161°
			1°	1°	1°

symmetry lies at $\theta \approx 150°$. Finally, Tuthill et al. (2001) stressed the importance of polarimetric measurements to determine the optical properties of the dust.

Polarimetric investigations of this star were started thirty years ago by Serkowski (1970) and since that time some 10 papers on the polarimetry of R Aqr have been published. Because we are planning to discuss the polarimetric characteristics of this object in more detail in a separate paper, we present here only a brief commentary on our data, without comparison with previously published results.

Our entire dataset is plotted in the *qu*-plane in Figs. 4a–c. As is evident from these figures, polarimetric variability is present on short time-scales (even during one night) and on intermediate time-scale (days). Moreover, the data in the VR_C bands are clustered in separate regions of the *qu*-diagram for the 1994 and 1995 runs. Assuming the distance derived from the Hipparcos parallax to be $197.2^{+33.3}_{-75.5}$ pc, we estimate an IS component of polarization in the V-band as $P_{is} = 0.16\% \pm 0.02\%$ at $\theta_{is} = 145° \pm 3°$. A change in the position angle for different passbands is evident both during each of our observing seasons, and between them, but this behaviour is not seen in the I_C-band (see Table 5).

For all dates when 5-colour polarimetry was carried out, the degree of polarization increases towards shorter wavelengths, reaching the values 4%–7% in the B and U bands (see Fig. 5). On JD 9576 we obtained two 5-colour

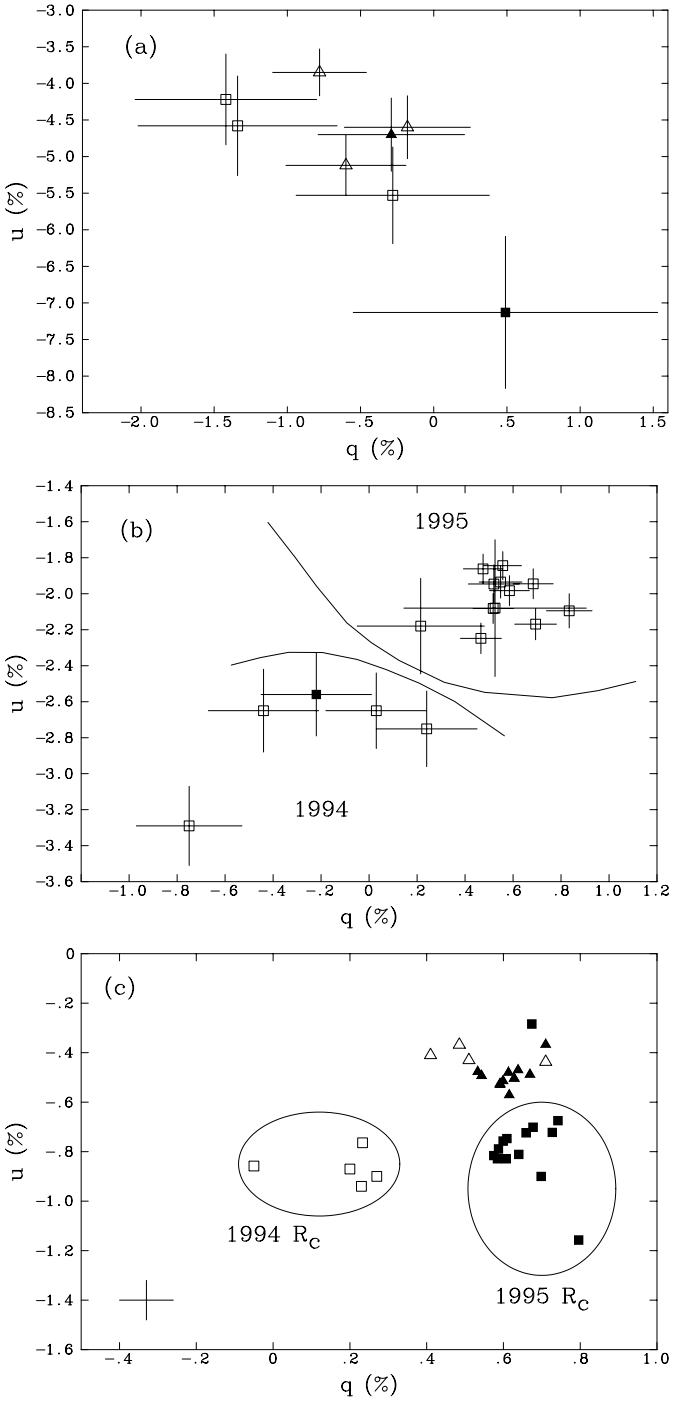

Fig. 4. a) *qu* diagram for R Aqr in the *UB* bands. Squares, U-band; triangles, B-band. Open symbols, data obtained with 20″ aperture; filled symbols with a 10″ filter. **b)** as **a)** but for the V band. **c)** as **a)** but for the $R_C\,I_C$ bands. Open symbols, 1994 data; filled symbols, 1995 data. Squares, R_C-band; triangles, I_C-band. A typical error bar is shown at lower left.

observations using a different size aperture. We note that the polarization degree detected with the smaller aperture in the U and B bands is significantly higher than that detected with a larger aperture. No differences due to aperture size used were detected in the VR_CI_C bands. This result clearly indicates the strong influence of the

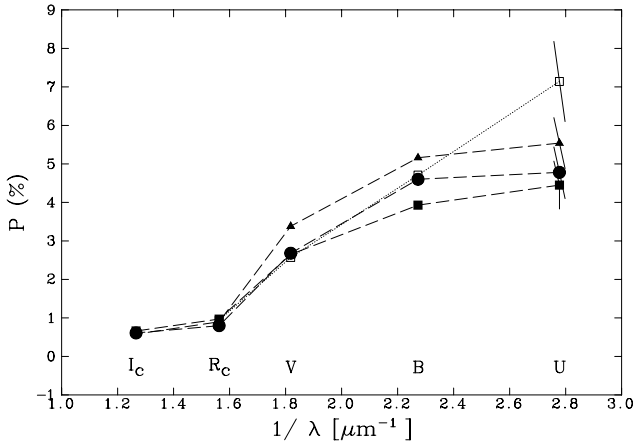

Fig. 5. Wavelength-dependence of polarization for R Aqr. Dashed lines and filled symbols, data obtained using 20″ aperture on JD...575 (triangles), JD...576 (squares), JD...579 (circles). Dotted line and open squares, data obtained using 10″ aperture on JD 576. Error bars are omitted from all but *U*-band data for clarity.

nebula on the polarimetric data in the ultraviolet. The wavelength-dependence of polarization for observations with the smaller aperture is well-described by the law $P \propto \lambda^{-2.5}$. The independence of polarization on aperture size in the red, together with the changes of θ in the different bands, indicate that different agents in the CS environment of R Aqr are responsible for the polarization at different wavelengths. All our observations were conducted when the object was at minimum brightness (light curve phases ranging between 0.45 and 0.57, taking $\phi = 0$ is at maximum light). Finally we note that, in a few cases, R Aqr shows detectable circular polarization, which occasionally reaches the value ∼0.3–0.4% (see Table 4: JDs 9918, 9929) with changes of a sign on a time-scale of of a few days. We defer a detailed discussion of this object to a separate paper.

5. Concluding remarks

(i) We have presented new measurements of linear and circular polarization for RS CVn and Mira variables, and have analysed their polarimetric variability on different time scales, from hours to a year. There is evidence, from polarimetric variability and from the wavelength-dependence of polarization, for the presence of intrinsic polarization for each of the programme stars.

(ii) We note the importance of taking into account IS polarization, and we have determined the IS component of polarization for all the stars.

(iii) For the RS CVn variables in our study we find $P(\lambda) \propto \lambda^{-4}$, suggesting that the polarization arises from scattering off small dust particles or molecules in the CS environment.

(iv) For the Mira variables, we find a flatter wavelength-dependence, $P \propto \lambda^{-2.5}$, but in the case of R Cet, the polarization increases to the red. The degree of polarization, and its wavelength-dependence, is aperture-dependent in the case of the symbiotic Mira R Aqr.

(v) Although all the objects in our study showed polarimetric variability on different time scales, only for IM Peg were these variations possibly linked with photometric period.

(vi) In combination with previously-published data, we conclude that the RS CVn and the Mira variables in this study show evidence of large polarimetric variability at wavelengths shorter than 0.5 μm, whereas the level of polarization is more stable in the red.

The large changes in the degree of polarization in the *UB* bands, in contrast to relatively stable polarization in the red, may be the result of episodic formation and/or destruction of small dust particles in the CS environments. Although we cannot exclude that, for some objects, polarization at the lower photometric state is due to the presence of spots on the stellar surface, in this case the wavelength-dependence of polarization must show monotonic *decrease* of P with λ. The shape of the wavelength-dependence will range from $P \propto \lambda^{-1.5}$ to approximately flat, depending on the star/spot temperature difference and a fraction of total spotted area (see Schwarz & Clarke 1984). With the exception of R Cet, most of our programme stars show a decrease of P with increasing λ, consistent with a steeper wavelength-dependence.

We note below the importance of the following points in future investigations and analysis of the polarization of evolved stars:

(i) Polarimetric monitoring during an entire photometric cycle, at different states of brightness, can help to establish (or otherwise) a link between polarization and pulsation or orbital periods, thus helping to resolve the problem of the mechanism(s) of polarization. This is also important to study the distribution of CS matter (blobs, clumps, clouds etc.) in the CS environment.

(ii) With the same aim, the wavelength-dependence of polarization should be investigated at different photometric phases.

(iii) The detection of circular polarization and its variability during pulsation or rotation periods can give at least upper limits on the magnetic field in these systems.

These projects do not require access to large telescopes, and can easily be carried out, at least for short-period binaries.

Acknowledgements. We acknowledge generous awards of time by the allocation panel of the SAAO, and the Particle Physics and Astronomy Research Council (PPARC) for the provision of travel funds. We also thank Dr. D. Buckley for support at SAAO. RVY was supported by a Royal Society Grant, and by grants RFBR 02-02-16543 and INTEGRACIIA. This work made use of the *SIMBAD* database.

References

Berdyugina, S. V., Ilyin, I., & Tuominen, I. 1999, A&A, 347, 932

Brandi, E., Garcia, L. G., Piirola, V., Scaltriti, F., & Quiroga, C. 2000, A&AS, 145, 197

Chinarova, L. L., Andronov, I. L., & Schweitzer, E. 1996, OAP, 9, 100

Clarke, D., Smith, R. A., & Yudin, R. V. 1998, A&A, 336, 604

Clarke, D., & Stewart, B. G. 1986, Vistas Astron., 29, 27

Cropper, M. 1985, MNRAS, 212, 709

Donati, J.-F., Semel, M., Carter, B. D., Rees, D. E., & Cameron, A. C. 1997, MNRAS, 291 658

Donati, J.-F., Semel, M., & Rees, D. E. 1992, A&A, 265, 669

Dulk 1985, ARA&A, 23, 169

Groenewegen, M. A. T., & Whitelock, P. A. 1996, MNRAS, 281, 1347

Hall, J. C., & Ramsey, L. W. 1994, AJ, 107, 1149

Han Won-Yong, & Kim Tu-Hwan 1988, PASP, 100, 964

Heiles, C. 2000, AJ, 119, 923
`http://vizier.u-strasbg.fr/vis-bin/Cat?II/226`

Hollis, J. M., Pedelty, J. A., & Lyon, R. G. 1997, ApJ, 482, L85

Hollis, J. M., Pedelty, J. A., Forster, J. R., et al. 2000, ApJ, 543, L81

Hollis, J. M., Boboltz, D. A., Pedelty, J. A., White, S. M., & Forster, J. R. 2001, ApJ, 559, L40

Hsu, J., & Breger, M. 1982, ApJ, 262, 732

Jassur, D. M. Z., & Kermani, M. H. 1994, Ap&SS, 219, 35

Kalimeris, A., Mitrou C. K., Doyle, J. G., Antonopoulou, E., & Rovithis-Livaniou, H. 1995, A&A, 293, 371

Karovska, M., McCarthy, D. W., & Chistou, J. C. 1994, in Eighth Cambridge Workshop on Cool Stars, Stellar Systems, and the Sun, ed. J.-P. Caillault (San Francisco: ASP), ASP Conf. Ser., 64, 652

Kholopov, P. N., Samus, N. N., Frolov, M. S., et al. 1998, The Combined General Catalogue of Variable stars
`http://vizier.u-stasbg.fr/II/214A`

Kruszewski, A., Gehrels, T., & Serkowski, K. 1968, AJ, 73, 677

Lanza, A. F., Rodono, M., Mazzola, L., & Messina, S. 2001, A&A, 376, 1011

Liu Xue-Fu, & Tan Hue-Song 1987, Acta Astr. Sin., 28, 139

McCall, A., & Hough, J. H. 1980, A&AS, 42, 141

Montesinos, B., Giménez, A., & Fernández-Figueroa, M. J. 1988, MNRAS, 232, 361

Perryman, M. A. C., Lindegren, I., Kovalevsky, J., et al. 1997, A&A, 323, 49
`http://vizir.u-strasbg.fr/viz-bin/Cat?I/239`

Pfeiffer, R. J. 1979, ApJ, 232, 181

Scaltriti, F., Piirola, V., Coyne, G. V., et al. 1993a, A&AS, 102, 343

Scaltriti, F., Busso, M., Ferrari-Toniolo, M., et al. 1993b, MNRAS, 264, 5

Schulte-Ladbeck, R. E. 1985, A&A, 142, 333

Schulte-Ladbeck, R. E., & Magalhaes, A. M. 1987, A&A, 181, 213

Schulte-Ladbeck, R. E., Aspin, C., Magalhaes, A. M., & Schwarz, H. E. 1990, A&AS, 86, 227

Schwarz, H. E., & Clarke, D. 1984, A&A, 132, 370

Serkowski, K., & Shawl, S. J. 2001, AJ, 122, 2017

Serkowski, K. 1966a, ApJ, 155, 857

Serkowski, K. 1996b, IBVS, 141

Serkowski, K. 1970, ApJ, 160, 1083

Shawl, S. J. 1975a, AJ, 80, 595

Shawl, S. J. 1975b, AJ, 80, 602

Sowell, J. R., Hughes, S. B., Hall, D. S., & Howard, B. A. 2001, AJ, 122, 1965

Tuthill, P. G., Danchi, W. C., Hale, D. S., Monnier, J. D., & Townes, C. H. 2001, ApJ, 534, 907

Welty, A. D., & Ramsey, L. W. 1995, AJ, 109, 2187

Whitelock, P. A. 1987, PASP, 99, 573

Wilson, L. A., Garnavich, P., & Mattei, J. A. 1981, IBVS, 1961

Vasil'ev, V. P., Vasil'ev, S. V., Zhurba, V. I., & Shakhovskoj, N. M. 1993, SvA, 37, 667

Yudin, R. V., & Evans, A. 1998, A&AS, 131, 401